# Structural polymorphism of DNA-dendrimer complexes

Heather M. Evans,[1] A. Ahmad,[1] K. Ewert,[1] T. Pfohl,[1,*] A. Martin-Herranz,[1,†] R. F. Bruinsma,[2] and C. R. Safinya[1,‡]

[1]*Materials Department, Physics Department, and Biomolecular Science and Engineering Program, University of California, Santa Barbara, California 93106, USA*

[2]*Department of Physics and Astronomy, University of California, Los Angeles, California, 90095, USA and Instituut-Lorentz/LION, Universiteit Leiden, 2300 RA, Leiden, The Netherlands*

(Received 12 March 2003; published 11 August 2003)

DNA condensation *in vivo* relies on electrostatic complexation with small cations or large histones. We report a synchrotron x-ray study of the phase behavior of DNA complexed with *synthetic* cationic dendrimers of intermediate size and charge. We encounter unexpected structural transitions between columnar mesophases with in-plane square and hexagonal symmetries, as well as liquidlike disorder. The isoelectric point is a locus of structural instability. A simple model is proposed based on competing long-range electrostatic interactions and short-range entropic adhesion by counterion release.

DOI: 10.1103/PhysRevLett.91.075501 PACS numbers: 61.30.Eb, 61.30.St, 61.10.Eq

DNA condensation attracts wide interest from physicists, biologists, and biomedical gene therapy researchers [1]. The primary mechanism for DNA compaction is the electrostatic complexation of the negatively charged DNA chains with *polyvalent cations*. Naturally occurring condensation agents can be small trivalent and tetravalent cations, such as spermine and spermidine [2], encountered in bacteria, or the much larger histone proteins encountered in eukaryotic cell nuclei [3](histones are cylindrical with diameter $\approx 10$ nm and charge $\approx +200e$). Fundamental interest in DNA condensation was stimulated by the fact that small-cation DNA condensation cannot be understood within the classical Poisson-Boltzmann (PB) mean-field theory of aqueous electrostatics, but requires instead a description that includes effective *attraction* between like-charged DNA chains mediated by both short-range correlations and thermal fluctuations [4].

There are marked differences between the two forms of DNA condensation. Small cation-DNA complexes are ordered DNA bundles [5] with in-plane hexagonal symmetry [6]. At the macroscopic level, they can be considered as a *columnar mesophase*. On the other hand, DNA complexation with histones results in a "beads-on-a-string" structure with the DNA chain wrapping 1.75 times around each histone [3]. In this Letter we report a structural study of the complexation of DNA with "model histones" that are, in terms of size and charge, *intermediate* between the two canonical condensation agents. The model histones were dendrimer molecules [7] formed by the successive addition of identical monomer units into a treelike primary structure. The number of iterations $G$ can be controlled with great precision, resulting in highly monodisperse spherical particles. Dendrimer-DNA complexes, which have been studied as possible vectors for nonviral gene delivery [8], are commonly assumed to adopt the beads-on-a-string morphology [6,9], but when we examined them by synchrotron x-ray diffraction methods we encountered instead a unique and fascinating sequence of columnar mesophases.

We studied the condensation of DNA with cationic polypropylene(imine) (PPI) dendrimers [10] having a "bare" positive charge of $62e$ ($G = 4$) and $126e$ ($G = 5$), and a hydrodynamic radius $R$ of 1.6 and 2 nm, respectively [11]. Characteristic synchrotron x-ray scattering profiles [12] are shown in Fig. 1. For the $G4$-DNA system [Fig. 1(a)], we encounter three distinct structures as a function of the mixing ratio $N/P$. Here, $N$ is the number of positive amine charges of the dendrimers (assuming full protonation) and $P$ is the number of negative phosphate charges of the DNA backbone. The bottom section compares for $N/P = 1$ the scattering profile of a $G4$-DNA complex with that of a classical small-cation/DNA complex (10m$M$ of the trivalent cation spermidine). In both cases, we obtain a single well-defined diffraction peak with peak position $q_0$ close to 0.24 Å$^{-1}$, consistent with earlier diffraction studies [5] on spermidine-DNA complexes. Spermidine condensed DNA has a hexagonal bundle structure with lattice constant $a_H = 4\pi/\sqrt{3}q_0$ of 3.0 nm, the effective diameter of condensed $B$-DNA [13]. The $G4$-DNA complex is likely to have for $N/P = 1$ the same structure ("$H'$ phase"), but in the absence of well-defined higher-order diffraction peaks we cannot rule out a distorted hexagonal structure.

For increasing $N/P$ ratio, the peak position shifts to significantly lower $q$ values and a second diffraction peak $q_1$ appears. Surprisingly, for $N/P = 5$ [see middle section of Fig. 1(a)], the ratio $q_1/q_0 = 1.414 \pm 0.002$ of the two peak positions is definitely *not consistent* with either that of the hexagonal bundle structure (in which case $q_1/q_0 = \sqrt{3}$) or with the lamellar organization that characterizes for instance DNA-lipid complexes [14](in which case $q_1/q_0 = 2$). By elimination, we found only one consistent assignment for the peak positions over the measured $q$ range, namely, that of a two-dimensional (2D) square unit

  

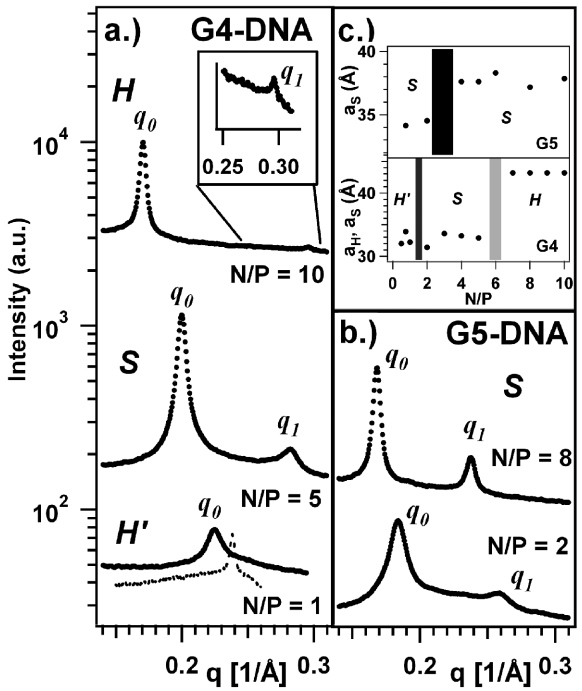


FIG. 1. (a),(b) X-ray scans as a function of the PPI-DNA charge ratio $N/P$ for $G4$-DNA (a) and $G5$-DNA (b) complexes. Dashed line in (a) is the scattering profile for a DNA/small-cation hexagonal bundle ($H'$ phase, 10m$M$ spermidine). The ratio $q_1/q_0$ equals $\sqrt{2}$ for square symmetry ($S$ phase) and $\sqrt{3}$ for hexagonal symmetry ($H$ phase). (c) Lattice constants of the $G4$-DNA (bottom) and $G5$-DNA (top) complexes as a function of $N/P$. Dark gray bars indicate the isoelectric point. The light gray bar indicates the $S$-to-$H$ phase transition.

cell with $q_1/q_0 = \sqrt{2}$ and a lattice constant $a_S = 2\pi/q_0$ of 3.4 nm ("$S$ phase"). Yet, for $N/P = 10$ [top section of Fig. 1(a)] the ratio of peak positions $q_1/q_0 = 1.73 \pm 0.008$ *is* consistent with a 2D hexagonal unit cell, now with $a_H$ equal to 4.4 nm. A well-defined $S$-to-$H$ structural phase transition occurs at $N/P = 6$. The $G5$-DNA system [Fig. 1(b)] is much simpler: for all measured $N/P$ values we obtain two diffraction peaks with the peak position ratio $q_1/q_0 = 1.411 \pm 0.005$ of the $S$ phase. However, the $S$ phase lattice constant $a_S = 2\pi/q_0$ undergoes a sharp increase near $N/P = 3$. Figure 1(c) shows the dependence of the lattice constants on the $N/P$ ratio for both $G4$ and $G5$ complexes.

The fact that the peak positions can be indexed only to a 2D unit cell suggests a columnar organization of PPI-DNA complexes. To confirm this, we carried out cross-polarized microscopy of the $S$ and $H$ phases. Both phases are birefringent (see Fig. 2), indicating that they are liquid-crystalline mesophases. Microscopy revealed that the aggregates had the morphology of flat or twisted threadlike ribbon structures, which is consistent with a columnar mesophase.

Figure 3 shows the proposed 2D unit cell of the $S$ and $H$ structures. The centers of the dendrimers are placed on

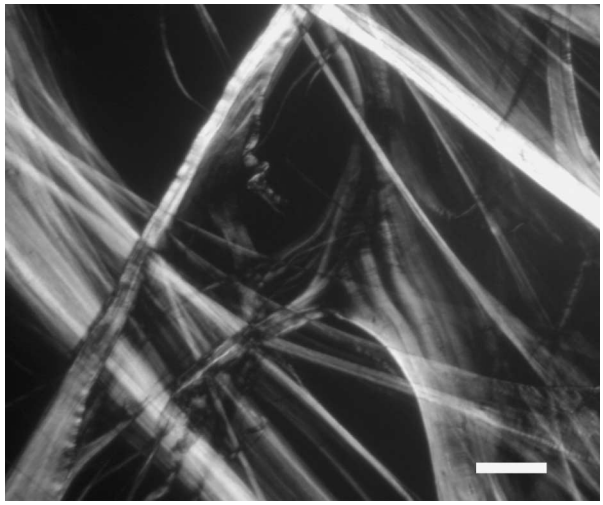

FIG. 2. Cross-polarized microscopy of $G4$-DNA complexes with $N/P = 10$. The individual threads consist of aligned columnar condensates (scale bar 0.1 mm).

symmetry sites of the interstitial regions separating the DNA columns. We assigned a 2.0 nm hard-core diameter to the DNA columns and the hydrodynamic radius $R$ to the dendrimers. Note the overlap of the dendrimers with the DNA cores in both the $S$ and $H$ phases and the dendrimer-dendrimer overlap in the $H$

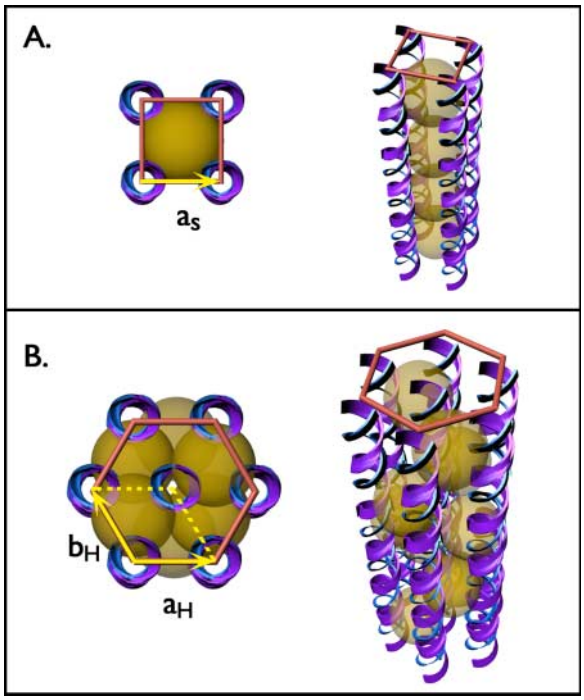


FIG. 3 (color online). Quasi-2D unit cells. DNA rods are drawn as helices. Dendrimers (solid circles) are centered on the symmetry sites of the interstitial regions for the (a) $S$ and (b) $H$ phases of $G4$. The $H$ phase contains two dendrimer columns per unit cell; the staggered arrangement is hypothetical.

phase (dendrimer-dendrimer repulsion is likely to stabilize the $S$ over the $H$ phase). In order to analyze the competition between the $S$ and $H$ structures, we first applied the well-established method [6] of using classical Debye-Huckel (DH) theory to compute the interaction between macroions while assigning renormalized, effective charges computed with Poisson-Boltzmann theory. We treated both the DNA molecules and the chains of dendrimer molecules as cylindrical macroions, with (effective) charges per unit length of $-\lambda^*$ for the DNA case [15] and $+Z^*n$ for the dendrimer case ($n$ is the number of dendrimers per unit length per column and $Z^*$ is the renormalized dendrimer charge). The DH free energy $f^{\mathrm{DH}}(n)$ per unit length of DNA equals

$$f^{\mathrm{DH}}(n) \cong \tilde{c}_{S,H}\frac{\lambda^{*2}}{\varepsilon_w}\ln(\kappa_D a_{S,H}) + \hat{c}_{S,H}\frac{(\lambda^* - Z^*n)^2}{\varepsilon_w(\kappa_D a_{S,H})^2}. \quad (1)$$

Here, $\varepsilon_w \approx 80$ is the dielectric constant of water, $\kappa_D$ is the Debye parameter (i.e., the inverse screening length), and $c_{S,H}$ stands for numerical factors. The first term of Eq. (1) is the *cohesive* energy of a charge-neutral complex. For such an "isoelectric" complex, $n$ has to equal $n_{\mathrm{iso}} = \lambda^*/Z^*$. An isoelectric columnar complex can be viewed as a (quasi-) 2D *ionic crystal*. The effective 2D Madelung constant of this ionic crystal is the numerical factor $\tilde{c}$ in Eq. (1), which equals approximately 2 for the $S$ phase and $3/2$ for the $H$ phases. The second term of Eq. (1) describes the significant free energy cost associated with deviations from the isoelectric point (IP). According to Eq. (1) the most stable structure should be the isoelectric $S$ phase (just as 3D salt solutions crystallize out as charge-neutral ionic crystals with a cubic structure). This obviously disagrees with our observations. The PPI-DNA complexes undergo charge reversal at an IP which, for $G4$, is near $N/P = 1.8$ and near $N/P = 3$ for $G5$ (zeta potential, not shown). According to Fig. 1(c), both IPs are characterized by a pronounced structural *instability*, which appears to directly contradict the structure of the DH free energy.

An important correction to the DH description is the so-called "counterion release" phenomenon [16]. For the present case, counterion release means that when a dendrimer is placed in direct contact with a DNA molecule, a certain number of the "Manning-condensed" positive counterions of DNA [15] can be released into solution. The ensuing gain in entropy produces a short-range *adhesive interaction* between the two macroions. Short-range adhesive interaction favors a hexagonally packed structure over square symmetry so electrostatic adhesion and cohesion impose conflicting structural requirements. Finally, macroion complexation by counterion release is characterized by instability of the IP: a charge-neutral macroion complex with no counterions cannot be in electrochemical equilibrium with free macroions in solutions that carry condensed counterions [17]. This IP instability was observed for DNA-lipid complexes [18].

In order to be able to test this interpretation, we examined the effect of *added salt*. When we combine the Hertz theory for short-range contact adhesion [19] with the PB theory of counterion release [20], we obtain a DNA-dendrimer binding energy $\epsilon(\kappa_D Z)$ that depends on the Debye parameter $\kappa_D$ as $[-\ln(\kappa_D d_{\mathrm{DNA}})]^{5/3}/K^{2/3}$, with $K$ the elastic modulus of the dendrimer [21] and $d_{\mathrm{DNA}}$ the DNA diameter. Because the DH cohesion energy depends on $\kappa_D$ as $-\ln(\kappa_D a_{S,H})$ [see Eq. (1)], the addition of salt should weaken *both* cohesive and adhesive contributions to the free energy—since $\kappa_D^2$ is proportional to the added salt concentration—but short-range adhesion by counterion release should be suppressed more effectively than cohesion due to long-range Coulomb interactions.

Figure 4(d) shows the measured phase diagram as a function of salt concentration (NaCl) and $N/P$ ratio. The $S$ phase remains stable—at lower $N/P$ ratios—for salt concentrations as high as 200m$M$, and the scattering profiles do not show a significant dependence on salt concentration [Figs. 4(a)–4(c), bottom row, with $N/P = 2$]. However, the $H$ phase is unstable for salt concentrations above 100m$M$. The top row of Figs. 4(a)–4(c) shows

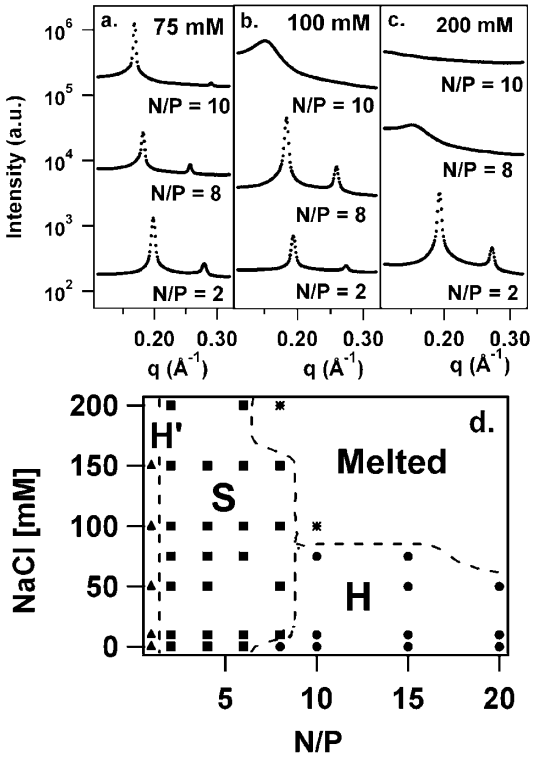


FIG. 4. X-ray scans of $G4$-DNA complexes with NaCl. (a) For 75m$M$, the $S$-to-$H$ transition is shifted to a higher $N/P$ value than without salt. The lattice constant increases with $N/P$. (b) For 100m$M$, the $S$ phase remains stable but long-range, in-plane positional order of the $H$ phase is lost. (c) For 200m$M$, the melting transition takes place earlier ($N/P = 8$). (d) The full phase diagram as a function of salt concentration and $N/P$ ratio.

that for $N/P = 10$ the diffraction peak first broadens at 100m$M$—indicating loss of long-range positional order—while at 200m$M$ salt the peak has disappeared altogether [though for $N/P = 8$ it is still visible; see Fig. 4(c)]. The $S$, $H$, and molten phases come together at a multicritical point near $N/P = 10$ and 100m$M$ salt concentration.

This phase diagram is in good—albeit qualitative—agreement with the proposed interpretation: increased screening of the electrostatic interaction destabilizes the $H$ phase but affects the $S$ phase only weakly. The model also provides insight into why only the $S$ phase appears for $G5$ dendrimers: the dendrimer elastic modulus $K$ should increase with the generation $G$ due to increased steric hindrance. Since $\epsilon \propto 1/\mathrm{K}^{2/3}$, the weakening of the adhesion energy would account for the stabilization of the $S$ phase with increasing $G$ number.

In summary, PPI-DNA complexes are columnar mesophases consisting of arrays of DNA rods intercalated with dendrimers. The classical beads-on-a-string model is not appropriate, probably because the charge of the dendrimers is too weak—and their size too small—to allow the wrapping of DNA around the dendrimers. On the other hand, the small-cation hexagonal bundling scenario is also not appropriate in view of the appearance of columnar structures with *square* symmetry. We encounter a competition between square and hexagonal symmetry for the $G4$ complexes. We propose that the basic underlying mechanism is the competition between long-range electrostatic cohesion and short-range electrostatic adhesion by counterion release. The appearance of a structural instability at the IPs supports this conclusion. Final confirmation could be by direct measurement of the counterion concentration in solution near the phase boundaries, as was done for DNA-lipid complexes [22].

This work was supported by National Institutes of Health Grant No. GM-59288 and National Science Foundation Grants No. DMR-0203755 and No. CTS 0103516. Support was also provided by Los Alamos National Laboratory–UCSB Grant No. 45909-0012-2P. The Stanford Synchrotron Radiation Laboratory is supported by the U.S. Department of Energy. The Materials Research Laboratory at UCSB is supported by NSF Grant No. DMR-0080034.

*Present address: Department of Applied Physics, University of Ulm, D-81241 Ulm, Germany.
†Present address: Unilever R&D, Manuel de Falla 7, 28036 Madrid, Spain.
‡Electronic address: safinya@mrl.ucsb.edu

[1] *Pharmaceutical Perspectives in Nucleic Acid-Based Therapeutics*, R. I. Mahato and S. W. Kim (Taylor & Francis, London, 2002).
[2] V. A. Bloomfield, Curr Opin Struct Biol **6**, 334 (1996); E. Raspaud, M. Olvera de la Cruz, J. L. Sikoray, and F. Livolant, Biophys. J. **74**, 381 (1998).
[3] J. Widom, Annu. Rev. Biophys. Biomol. Struct. **27**, 285 (1998).
[4] For a review, see W. Gelbart, R. Bruinsma, P. Pincus, and V. A. Parsegian, Phys. Today, **53**, No. 9, 38 (2000).
[5] J. Pelta, Jr., D. Durand, J. Doucet, and F. Livolant, Biophys. J. **71**, 48 (1996).
[6] See, for instance, N. V. Hud and K. H. Downing, Proc. Natl. Acad. Sci. U.S.A. **98**, 14 925 (2001).
[7] D. Tomalia, Sci. Am. **272**, 62 (1995).
[8] J. F. Kukowska-Latallo, A. U. Bielenska, J. Jonson, R. Spindler, D. A. Tomalia, and J. R. Baker, Jr., Proc. Natl. Acad. Sci. U.S.A. **93**, 4897 (1996).
[9] W. Chen, N. J. Turro, and D. Tomalia, Langmuir **16**, 15 (2000); V. Kabanov, V. G. Sergeyev, and O. A. Pyshkina, Macromolecules **33**, 9587 (2000).
[10] The PPI dendrimers were used as received from Aldrich (DAB-Am-32, $FW = 3514$, and DAB-Am-64, $FW = 7168$). PPI-DNA complexes were made using highly polymerized calf thymus DNA (lyophilized, from USB) in water at 10 mg/m$l$. Experiments were at room temperature.
[11] A. Topp, B. Bauer, T. J. Prosa, R. Scherrenberg, and E. J. Amis, Macromolecules **32**, 8923 (1998).
[12] Beam line 4-2 of Stanford Synchrotron Radiation Laboratory using $E = 8.98$ keV.
[13] D. C. Rau and V. A. Parsegian, Biophys. J. **61**, 260 (1992).
[14] J. Radler, I. Koltover, T. Salditt, and C. R. Safinya, Science **275**, 810 (1997).
[15] Within Poisson-Boltzmann theory $\lambda^* = l/l_B$, $l_B = e^2/\varepsilon_w k_B T =$ (the Bjerrum length). F. Oosawa, Biopolymers **6**, 1633 (1968); G. S. Manning, J. Chem. Phys. **51**, 924 (1969).
[16] P. L. deHaseth, T. M. Lohman, and M. T. Record, Biochemistry **16**, 4783 (1977).
[17] R. Bruinsma, Eur. Phys. J. B **4**, 75 (1998).
[18] I. Koltover, T. Salditt, and C. R. Safinya, Biophys. J. **77**, 915 (1999).
[19] L. Landau and E. Lifshitz, *Theory of Elasticity* (Pergamom, New York, 1975), Ch. 9.
[20] S. Y. Park, R. F. Bruinsma, and W. M. Gelbart, Europhys. Lett. **46**, 454 (1999).
[21] $\mathrm{K} = 10^8$ N/m$^2$ for dendrimers. See V. V. Bessonov, N. K. Balabaev, and M. A Mazo, Russ. J. Phys. Chem. **76**, 1806 (1997).
[22] K. Wagner, D. Harries, S. May, V. Kahl, J. O. Radler, and A. Ben-Shaul, Langmuir **16**, 303 (2000).